



Activation of Galanin Receptor 1 with M617 Attenuates Neuronal Apoptosis via ERK/GSK-3 β /TIP60 Pathway After Subarachnoid Hemorrhage in Rats

Hui Shi¹ · Yuanjian Fang² · Lei Huang^{3,4} · Ling Gao⁴ · Cameron Lenahan⁴ · Takeshi Okada⁴ · Zachary D. Travis⁴ · Shucai Xie⁴ · Hong Tang⁴ · Qin Lu⁴ · Rui Liu⁴ · Jiping Tang⁴ · Yuan Cheng⁵ · John H. Zhang^{3,4,6} 

Accepted: 14 May 2021 / Published online: 4 June 2021
© The American Society for Experimental NeuroTherapeutics, Inc. 2021

Abstract

Subarachnoid hemorrhage (SAH) is a devastating cerebrovascular disease. Neuronal apoptosis plays an important pathological role in early brain injury after SAH. Galanin receptor 1 (GalR1) activation was recently shown to be anti-apoptotic in the setting of ischemic stroke. This study aimed to explore the anti-neuronal apoptosis effect of GalR1 activation after SAH, as well as the underlying mechanisms. GalR1 CRISPR and GalR1 selective agonist, M617, was administered, respectively. Extracellular-signal-regulated kinase (ERK) inhibitor (U0126) and glycogen synthase kinase 3-beta (GSK3- β) CRISPR were administered to investigate the involvement of the ERK/GSK3- β pathway in GalR1-mediated neuroprotection after SAH. Outcome assessments included neurobehavioral tests, western blot, and immunohistochemistry. The results showed that endogenous ligand galanin (Gal) and GalR1 were markedly increased in the ipsilateral brain hemisphere at 12 h and 24 h after SAH. GalR1 were expressed mainly in neurons, but expression was also observed in some astrocytes and microglia. GalR1 CRISPR knockdown exacerbated neurological deficits and neuronal apoptosis 24 h after SAH. Moreover, activation of GalR1 with M617 significantly improved short- and long-term neurological deficits but decreased neuronal apoptosis after SAH. Furthermore, GalR1 activation dysregulated the protein levels of phosphorylated ERK and GSK-3 β , but down-regulated the phosphorylated Tat-interactive protein 60 (TIP60) and cleaved caspase-3 at 24 h after SAH. GalR1 CRISPR, U0126, and GSK-3 β CRISPR abolished the beneficial effects of GalR1 activation at 24 h after SAH in rats. Collectively, the present study demonstrated that activation of GalR1 using M617 attenuated neuronal apoptosis through the ERK/GSK-3 β /TIP60 pathway after SAH in rats. GalR1 may serve as a promising therapeutic target for SAH patients.

Keywords M617 · GalR1 · Early brain injury · Neuronal apoptosis · Subarachnoid hemorrhage

Abbreviations

Gal Galanin;
GalR1 Galanin receptor 1
GalR2 Galanin receptor 2
GalR3 Galanin receptor 3

SAH Subarachnoid hemorrhage
ERK Extracellular signal-regulated kinase
MAPK Mitogen-activated protein kinase
GSK-3 β Glycogen synthase kinase-3 β
TIP60 Tat-interactive protein 60
CNS Central nervous system

Hui Shi and Yuanjian Fang contributed equally to this work.

✉ Yuan Cheng
chengyuan023@aliyun.com

✉ John H. Zhang
johnzhang3910@yahoo.com

¹ Department of Neurosurgery, Chongqing Medical University, Yongchuan Hospital, Yongchuan, Chongqing, China

² Department of Neurosurgery, School of Medicine, The Second Affiliated Hospital, Zhejiang University, Hangzhou, Zhejiang, China

³ Department of Neurosurgery, Loma Linda University, Loma Linda, CA, USA

⁴ Department of Physiology and Pharmacology, School of Medicine, Loma Linda University, Loma Linda, CA, USA

⁵ Department of Neurosurgery, Second Affiliated Hospital of Chongqing Medical University, Chongqing, China

⁶ Department of Neurosurgery and Anesthesiology, Loma Linda University Medical Center, Loma Linda, CA, USA

Introduction

Subarachnoid hemorrhage (SAH) has an annual global incidence of 2–22 per 100,000 people and is associated with high mortality and morbidity [1, 2]. Early brain injury (EBI), characterized as the pathophysiology change that occurs within 72 h after SAH, is considered the main contributor to the poor outcome of SAH patients [3, 4]. Therapeutic approaches targeting the pathological process of EBI benefit SAH outcomes [5, 6]. Neuronal apoptosis plays an important pathological role in EBI [7]. Therefore, inhibition of neuronal apoptosis is considered a promising treatment strategy to improve neurological deficits following SAH [8].

Galanin is a neuropeptide and co-transmitter that regulates neurotransmission in the peripheral and central nervous system (CNS) [9]. Early studies have focused on the function of galanin in mood disorder, drug addiction, inflammation, and diabetes [10, 11]. A recent *in vitro* study revealed that galanin has protective effects in high glucose-induced neuronal injury in dorsal root ganglion [12]. The galanin receptor family consists of three G protein-coupled receptors, galanin receptor 1 (GalR1), galanin receptor 2 (GalR2), and galanin receptor 3 (GalR3), which mediate multiple physiological roles of galanin in various tissues via different functional coupling and subsequent signaling pathways [13]. The knockdown of GalR1 increased cell apoptosis in colorectal cancer cells, but GalR2 activation promoted apoptosis in head and neck squamous cell carcinoma [14–16]. GalR1 activation reduced neuronal death in a rodent model of ischemic stroke [17] and kainic acid-induced excitotoxicity hippocampus injury [18]. However, the role of GalR1 in SAH remains unclear. Downstream signaling of GalR1 is activated through the mitogen-activated protein kinase (MAPK) family independently of protein kinase C [19]. In a study of squamous cancer cells, activated GalR1 could induce extracellular signal-regulated kinase 1/2 (ERK1/2) activation through the α i-subunit, thereby further inhibiting cyclin D-dependent proliferation [14]. Glycogen synthase kinase-3 β (GSK-3 β) is inactive when phosphorylated by ERK [20, 21]. Increased expression of pERK and pGSK-3 β caused the reduction of neuronal cell death [22, 23]. However, the expressions of phosphorylated ERK (pERK) and GSK-3 β were decreased after SAH in rat [22, 24]. Furthermore, recent work demonstrated that activation of Tat-interactive protein 60 (TIP60) at Ser86 by GSK-3 β induced cell death [25]. TIP60 Ser86 promotes p53-induced apoptotic protein activation, such as p53 upregulated modulator of apoptosis (PUMA) and Bcl-2-associated X protein (BAX) [26, 27]. Thus, the activation of ERK could reduce p53-mediated apoptosis [28, 29], possibly through inhibiting the GSK-3 β /TIP60 pathway.

Herein, we hypothesize that GalR1 activation induced by M617 attenuates neuronal apoptosis and improves neurological function via ERK/GSK-3 β /Tip60 pathway after SAH in rats.

Methods

Animals

A total of 248 adult male Sprague-Dawley (SD) rats, weighing 280–310 g, were used in this experiment. Animals were kept in an environment where food and water were freely available. The ambient temperature and humidity were monitored and controlled, with a light/dark cycle that alternated every 12 h. All operations and experimental procedures are approved by the Institutional Animal Care and Use Committee (IACUC) of Loma Linda University, and strictly in accordance with the requirements of the NIH animal use guidelines and ARRIVE guidelines (animal research: *in vivo* experiment report).

Experimental Designing

The experiment consists of 5 parts, as shown in Fig. 1.

Experiment 1. To determine the time course of endogenous galanin, GalR1, and GalR2 protein expressions in the ipsilateral (left) hemisphere at 3, 6, 12, 24, and 72 h after SAH. Cellular localization of GalR1 were examined in the brain at 24 h after SAH.

Thirty-six rats were randomly divided into six groups ($n = 6$ /group): Sham, SAH-3h, SAH-6h, SAH-12h, SAH-24h, and SAH-72h. Western blot analysis was used to evaluate protein expression levels of galanin, GalR1, and GalR2. Four additional rats in the Sham and SAH-24h groups ($n = 2$ /group) were used to examine brain cellular localization of GalR1 via double immunofluorescence staining with neuronal nuclei (NeuN, neuron marker), glial fibrillary acidic protein (GFAP, astrocyte marker), or calcium binding adaptor molecule 1 (Iba-1, microglia marker).

Experiment 2. To evaluate the knock-out effects of GalR1 or GalR2 on neuro-apoptosis in the ipsilateral (left) hemisphere at 24 h after SAH.

Fifty rats were randomly divided into 5 groups ($n = 10$ /group): Sham, SAH + PBS, SAH + Scramble CRISPR, SAH + GalR1 CRISPR(KO), and SAH + GalR2 CRISPR(KO). Modified Garcia score, Beam Balance test, and SAH grades were assessed at 24 h after SAH. Six rats of each group were randomly selected for western blot assessments of protein levels of GalR1, GalR2, P53, Bcl-2, and Bax in ipsilateral (left) hemisphere brain tissues. The other four rats of each group were used for terminal deoxynucleotidyl transferase dUTP (TUNEL) staining and Fluoro-Jade C staining to

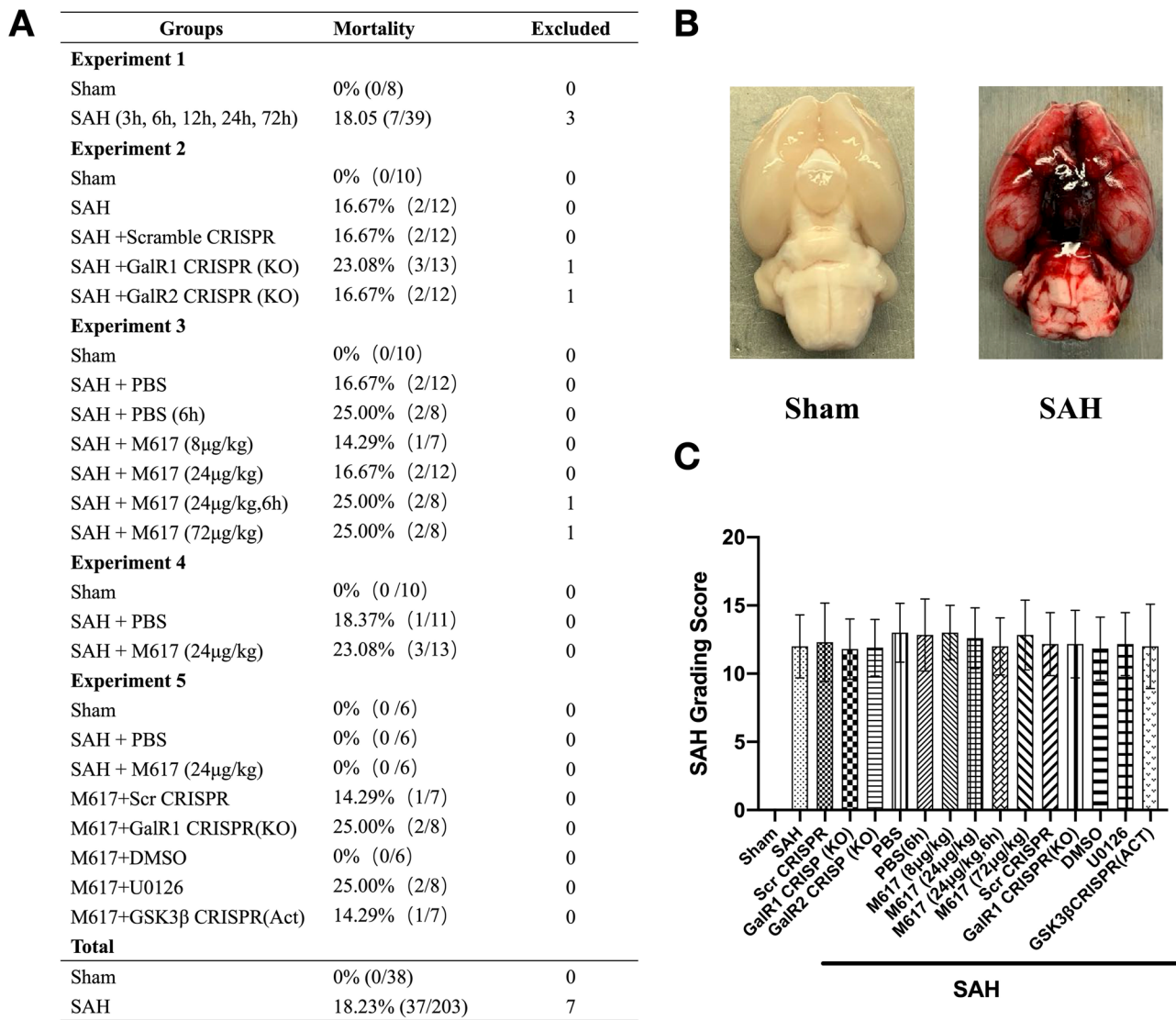


Fig. 1 Mortality and subarachnoid hemorrhage (SAH) grade. **(A)** Animal usage and mortality of all experiment groups. **(B)** Representative pictures showed that subarachnoid blood clots primarily pre-

sented around the circle of Willis in the rat brain at 24 h after SAH. **(C)** SAH grading scores of all SAH groups. Vehicle, phosphate-buffered saline (PBS)

evaluate the cell apoptosis and neuronal degeneration in the ipsilateral (left) hemisphere.

Experiment 3. To evaluate the short-term neuroprotective effect of GalR1 activation induced by M617

A total of 36 rats were randomly divided into five groups ($n = 6$ /group): Sham, SAH + PBS, SAH + M617 (8 μ g/kg), SAH + M617 (24 μ g/kg), and SAH + M617 (72 μ g/kg). M617 was dissolved in PBS and administered intranasally 1 h after SAH. Modified Garcia score, Beam Balance test, and SAH grades were measured at 24 h after SAH. Based on the neurological outcomes, M617 at 24 μ g/kg was determined to be the best dose, and was used for the following experiments: histology evaluation, delayed

treatment, long-term neurological outcomes, and mechanisms. An additional 12 rats were divided into three groups ($n = 4$ /group): Sham, SAH + PBS, and SAH + M617 (24 μ g/kg) to access the neuronal apoptosis in the ipsilateral (left) hemisphere at 24 h after SAH using TUNEL staining and Fluoro-Jade C staining.

To further validate the clinical relevance, another set of 12 rats were randomly divided into 2 groups ($n = 6$ /group): SAH + PBS (3 h) and SAH + M617 (3 h). M617 (24 μ g/kg) and PBS were administered at 3 h after SAH. Modified Garcia test, Beam Balance test, SAH grade, TUNEL staining, and Fluoro-Jade C staining were performed at 24 h after SAH.

Experiment 4. To evaluate the therapeutic effects of GalR1 activation induced by M617 on long-term neurological outcomes after SAH

Thirty rats were randomly assigned to three groups ($n = 10/\text{group}$): Sham, SAH + PBS, and SAH + M617. M617 (24 $\mu\text{g}/\text{kg}$) and PBS were administered 1 h after SAH. The Rotarod test was performed on days 7, 14, and 21 after SAH. Morris water maze was performed on days 22–27 after SAH. The rats were euthanized on day 28. In each group, 5 rats were randomly selected for Nissl staining and the other 5 rats were used for Fluoro-Jade C staining to assess the neuronal degeneration within hippocampus.

Experiment 5. To elucidate the neuroprotective mechanism of GalR1 activation induced by M617

Three groups, Sham, SAH + PBS, and SAH + M617, were shared with experiment 3. Another thirty rats were randomly divided into 5 groups ($n = 6/\text{group}$): SAH + M617 + Scr CRISPR, SAH + M617 + GalR1 CRISPR (KO), SAH + M617 + DMSO, SAH + M617 + U0126, and SAH + M617 + GSK-3 β CRISPR(Act). M617 (24 $\mu\text{g}/\text{kg}$) and PBS were administered at 1 h after SAH. Scramble CRISPR plasmid (Scr CRISPR), GalR1 CRISPR (KO) plasmid, or GSK-3 β CRISPR (Act) plasmid was administered intracerebroventricularly (icv) 48 h prior to SAH induction. DMSO or ERK inhibitor, U0126, were administered intraperitoneally (ip) 1 h prior to SAH induction. Ipsilateral hemispheres of the brains were collected for western blot analysis of the CalR1/ERK/GSK-3 β /Tip60 pathway after neurological assessments and SAH grading at 24 h after SAH.

SAH Model

Endovascular perforation model was used for SAH induction as previously described [30]. Under deep anesthesia (4% isoflurane for 2 min), rats were intubated and connected to a ventilator for mechanical ventilation. Isoflurane anesthesia was maintained at 3% during the surgery, and was reduced to 1.5% during SAH induction. A sharp 4–0 monofilament was inserted into the left external carotid artery to the internal carotid artery. Upon reaching the bifurcation of the anterior cerebral artery and the middle artery, the monofilament was further advanced, puncturing the vessel. Rats in the Sham groups underwent identical surgical procedures, but without vessel puncture. Peak inspiration pressure, respiratory rate, heart rate, skin pigmentation, and pedal reflex (firm toe pinch) were monitored throughout the operation. At the end of surgery, the tracheal tube was extubated, and the rats were allowed to rest on a heating pad in a cage, where they were monitored until complete recovery from anesthesia.

SAH Severity

The SAH severity was blindly assessed using the SAH grading scale as previously described [31]. Briefly, the basal cistern was divided into 6 areas; each area is assigned a score, ranging from 0 to 3, according to the amount of subarachnoid blood around the circle of Willis. Based on the sum of the scores from each of the 6 areas, each rat received an evaluation score ranging from 0 to 18. Since mild SAH is not associated with significant neurological deficits in this animal model [31], rats with mild SAH (SAH score < 9) were excluded from this study.

Drug Administration

Intranasal Administration

Intranasal administration was performed as previously described [30]. Briefly, the rat was placed in supine position under 3% isoflurane anesthesia. M617 (Tocris Bioscience, Minneapolis, MN, USA, Cat. No. 2697) was dissolved in PBS at a concentration of 3 $\mu\text{g}/\mu\text{l}$. The body weight of SD rats ranged from 280 to 310 g. Three different dosages (8, 24, or 72 $\mu\text{g}/\text{kg}$) in volumes of 0.75–7.44 μl were administered into the nares, alternating between left and right nares every 5 min, with maximal 4 μl administered in each naris until dosage administration was complete.

Intraperitoneal Administration

A 100 mg of U0126-EtOH was dissolved in 10-mL solvent of 10% DMSO, 40% PEG300, 5% Tween-80, and 45% saline. The body weight of SD rats ranged from 280 to 310 gram. U0126-EtOH at 30 mg/kg or vehicle in volumes 0.84 to 0.93 mL was administered via intraperitoneal injection in each rat at 1 h prior to SAH induction.

Intracerebroventricular Drug Administration

Intracerebroventricular injection (i.c.v) was performed as previously described [32, 33]. Briefly, rats placed in a stereotaxic frame were anesthetized with isoflurane anesthesia. The needle of a 10- μl Hamilton syringe (Hamilton Company Inc., Reno, NV) was inserted into the right lateral ventricle through a burr hole in the skull using the following coordinates relative to the bregma: 1.5 mm lateral, 0.9 mm caudal, and 3.3 mm below the horizontal plane of the skull.

In our study, GalR1 knockdown CRISPR plasmid (Santa Cruz Biotechnology, Dallas, TX, USA), GSK-3 β activate (Act) CRISPR plasmid (Santa Cruz Biotechnology, Dallas, TX, USA), or scrambled CRISPR plasmid (Santa Cruz Biotechnology, Dallas, TX, USA) was used to knockdown GalR1 and activate GSK-3 β gene expression. Resuspend 20

μ g of CRISPR plasmid in 100 μ l of ultrapure, sterile, DNase-free water. A total of 2 μ g of CRISPR plasmid in 10 μ l DNase-free water per rat was given i.c.v per rat at a rate of 1 μ L per min by a pump 48 h before SAH induction. To avoid cerebrospinal fluid and drug leakage, the needle remained in situ for 5 min after finishing injection, and was withdrawn slowly over 5 min. Bone wax was used to seal the hole on the skull immediately after complete withdrawal of the needle, and then the incision was sutured.

Short-term Neurological Performance

An investigator was assigned to assess the short-term neurobehavioral outcomes blindly at 24 h after modeling. Modified Garcia score with 18 points and Beam balance test with 4 points were used to evaluate the neurological deficits in each rat as previously described [34]. Lower scores represent worse neurological performance.

Long-term Neurological Performance

Rotarod Test

The rotarod test was used to assess sensorimotor coordination and balance on days 7, 14, and 21 after SAH as previously described [35]. The initial rotating speeds were 5 revolutions per minute (RPM) or 10 RPM, which then gradually accelerated at 2 RPM every 5 s. A photo beam circuit was used to record the duration that rats stayed on the accelerating rotating cylinder.

Morris Water Maze

The Morris water maze was applied on days 22–27 to assess spatial learning and memory capacities as previously reported [36]. The cue test, conducted on day 22 after modeling, was used as a control to evaluate any sensorimotor and/or motor dysfunction that may influence performance. The spatial water maze test was applied on days 23–27 after modeling. On day 28, the platform was removed from the water, and the rats underwent a 60-s probe trial. The Video Tracking System SMART-2000 (San Diego Instruments Inc., San Diego, CA) was used to trace the activities of the rats and their swim patterns, as well as to quantify the distance, latency, and swimming speed.

Histological Analysis

Rats were deeply anesthetized and transcardially perfused with 4 $^{\circ}$ C phosphate-buffered saline (PBS, 0.01 M, pH 7.4), followed by 10% formalin in a total volume of 100 mL. The whole brain was quickly collected, fixed in 4% formalin at 4 $^{\circ}$ C for 24 h, and then dehydrated in a 30% sucrose solution

for 72 h. After being embedded in OCT (Scigen Scientific Gardena, CA, USA) and frozen at -80° C, the 8–15- μ m coronal brain sections were sliced on a cryostat (LM3050S, Leica Microsystems, Bannockburn, Germany) and mounted on normal Poly-L-Lysine-coated slides for double immunofluorescence [37], TUNEL staining [37], Fluoro-Jade C staining, and Nissl staining [38].

Immunofluorescence Staining

Prepared slices were washed with 0.01 M of PBS three times for 10 min each, incubated in 0.3% Triton X-100 of PBS for 30 min at room temperature, and they were washed again three times for a period of 10 min in each wash. After being blocked with 5% donkey serum in 0.01M of PBS for 1 h at room temperature, the sections were incubated at 4 $^{\circ}$ C overnight with primary antibody including: anti-GalR1 (1:200, TA328849, Origene, Rockville, MD, USA), anti-NeuN (1:200, ab104224, Abcam, Cambridge, MA, USA), anti-GFAP (1:200, ab53554, Abcam, Cambridge, MA, USA), and anti-Iba-1 (1:200, ab5076, Abcam, Cambridge, MA, USA). Then, the sections were washed with 0.01M of PBS and incubated with appropriate fluorescence-conjugated secondary antibodies (1:500; Jackson ImmunoResearch Inc., West Grove, PA) for 1 h at room temperature. The slides were observed and photographed under a fluorescence microscope (DMi8; Leica Microsystems Inc., Germany).

Fluoro-Jade C Staining

Fluoro-Jade C staining was performed using Fluoro-Jade C Ready-to-Dilute Staining Kit (Biosensis, USA) to identify degenerating neurons according to the manufacturer's instructions. Four pictures were taken from the left temporal cortex and hippocampus of each rat under a fluorescence microscope to count Fluoro-Jade C-positive neurons. The average number of Fluoro-Jade C-positive neurons in the fields of each brain were presented as cells/mm², and calculated by Image-Pro Plus 6.0 software.

TUNEL Staining

To evaluate neuronal apoptosis, double staining of neuron marker, NeuN, and TUNEL staining was applied using In Situ Apoptosis Detection Kit (Roche, USA) at 24 h after modeling. Four pictures were taken from the left temporal cortex of each rat under a fluorescence microscope to count TUNEL-positive neurons. The average number of TUNEL-positive neurons in the fields of each brain was presented as the ratio of TUNEL-positive neurons (%).

Nissl Staining

Nissl staining was applied to assess hippocampus damage as previously reported [39]. The prepared 15- μm slices were selected to check the degenerating neurons in different hippocampal regions. The surviving neurons with normal morphology were counted, and the neuronal density loss was estimated within the hippocampal CA1 and CA3 regions.

Western Blot Analysis

The left hemisphere was used for Western blot analysis as previously described [40]. RIPA lysis buffer (sc-24948, Santa Cruz Biotechnology, TX, USA) was used to homogenize left hemispheres, and the supernatant was collected after centrifugation at 14,000 g for 30 min. Equal amounts of protein (30 μg) were loaded onto 8–12% SDS-PAGE gels, and then electrophoresed and transferred to nitrocellulose membranes. After electrophoresis, the protein was transferred to the nitrocellulose membrane. Membranes with proteins were blocked with 5% nonfat milk for 1 h at room temperature, followed by incubation for 6 h at 4 °C with the following antibodies: anti-galanin (1:1000, A00606-1, Boster Biological Technology, CA, USA), anti-GalR1 (1:2000, TA328849, OriGene Technologies, Inc. MD, USA), anti-GalR2 (1:500, LS-C805729, Lifespan Biosciences, WA, USA), anti-pERK1/2 (1:1000, sc-136521, Santa Cruz Biotechnology, USA), anti-ERK1/2 (1:1000, sc-514302, Santa Cruz Biotechnology, USA), anti-pGSK-3 β (1:2000, ab107166, Abcam, MA, USA), GSK-3 β (1:1000, ab131356, Abcam, MA, USA), anti-pTIP60 (1:500, bs-17096R, Bioss Antibodies Inc. MA, USA), anti-TIP60 (1:2000, ab23886, Abcam, MA, USA), anti-p53 (1:2000, ab131442, Abcam, MA, USA), anti-cleaved Caspase-3 (1:1000, D175, Cell Signaling Technology, MA, USA), anti-Bcl-2 (1:1000, ab59348, Abcam, MA, USA), anti-Bax (1:4000, ab182734, Abcam, MA, USA), and anti- β -actin (1:5000, sc-47778, Santa Cruz Biotechnology, TX, USA). On the second day, the membranes were incubated with the appropriate secondary antibody (1:5000, Santa Cruz Biotechnology Inc., TX, USA) at room temperature for 2 h. Immunoreactive bands were detected using a chemiluminescence reagent kit (ECL Prime; Amersham Biosciences Inc., Arlington Heights, IL) and quantified with densitometry with ImageJ software (NIH, Bethesda, MD).

Statistical Analysis

The data were presented as the mean \pm standard deviation (SD). GraphPad Prism (GraphPad Software, San Diego, CA, USA) was used to analyze all data. The normality of the

data was assessed using the Kruskal-Wallis test. One-way ANOVA followed by multiple comparisons with Tukey's post hoc test was used among different groups. Two-way repeated measures ANOVA with Tukey's post hoc test was performed to analyze long-term neurological functions. Statistical significance was considered at $P < 0.05$.

Results

Animal Use and Mortality

A total of 248 rats were used in this study. All rats survived in the Sham group. The overall mortality of SAH rats was 18.23% (37/203) without any significant difference among all SAH groups. Seven rats were excluded because of their mild SAH grades (Fig. 1A). Subarachnoid space was diffused with blood clots in SAH group, and no clots in sham group (Fig. 1B). There was no significant difference in the SAH grading score among the SAH groups (Fig. 1C).

Time Course of Endogenous Galanin, GalR1, and GalR2 Expressions in Ipsilateral Hemisphere and Cellular Localization of GalR1 After SAH

Western blot results showed that expression of endogenous Galanin began increasing at 3 h after SAH, and peaked at 12 h after SAH when compared with sham group ($P < 0.05$; Fig. 2A, B). The expression of endogenous GalR1 started increasing at 3 h after SAH, and peaked at 24 h after SAH when compared with sham group ($P < 0.05$; Fig. 2A, C). The expression of endogenous GalR2 did not demonstrate a statistical difference among sham and SAH groups ($P > 0.05$; Fig. 2A, D). Double immunofluorescence staining showed that GalR1 was expressed in neurons, astrocytes, and microglia in the ipsilateral basal cortex at 24 h after SAH (Fig. 2F).

CRISPR Knockdown of GalR1, but not GalR2, Increased the Expression of Apoptosis-related Proteins at 24 h After SAH

As shown in Fig. 3A–C, the expressions of GalR1 and GalR2 in rats with SAH were significantly reduced in the SAH + GalR1 CRISPR (KO) and GalR2 CRISPR (KO), respectively, when compared with SAH + Scr CRISPR group ($P < 0.05$). No statistical difference was found between the SAH + Scr CRISPR and the SAH groups ($P > 0.05$).

The expressions of apoptosis-related protein, P53, and pro-apoptotic protein, Bax, were markedly elevated in the ipsilateral cerebral hemisphere after SAH, which was further

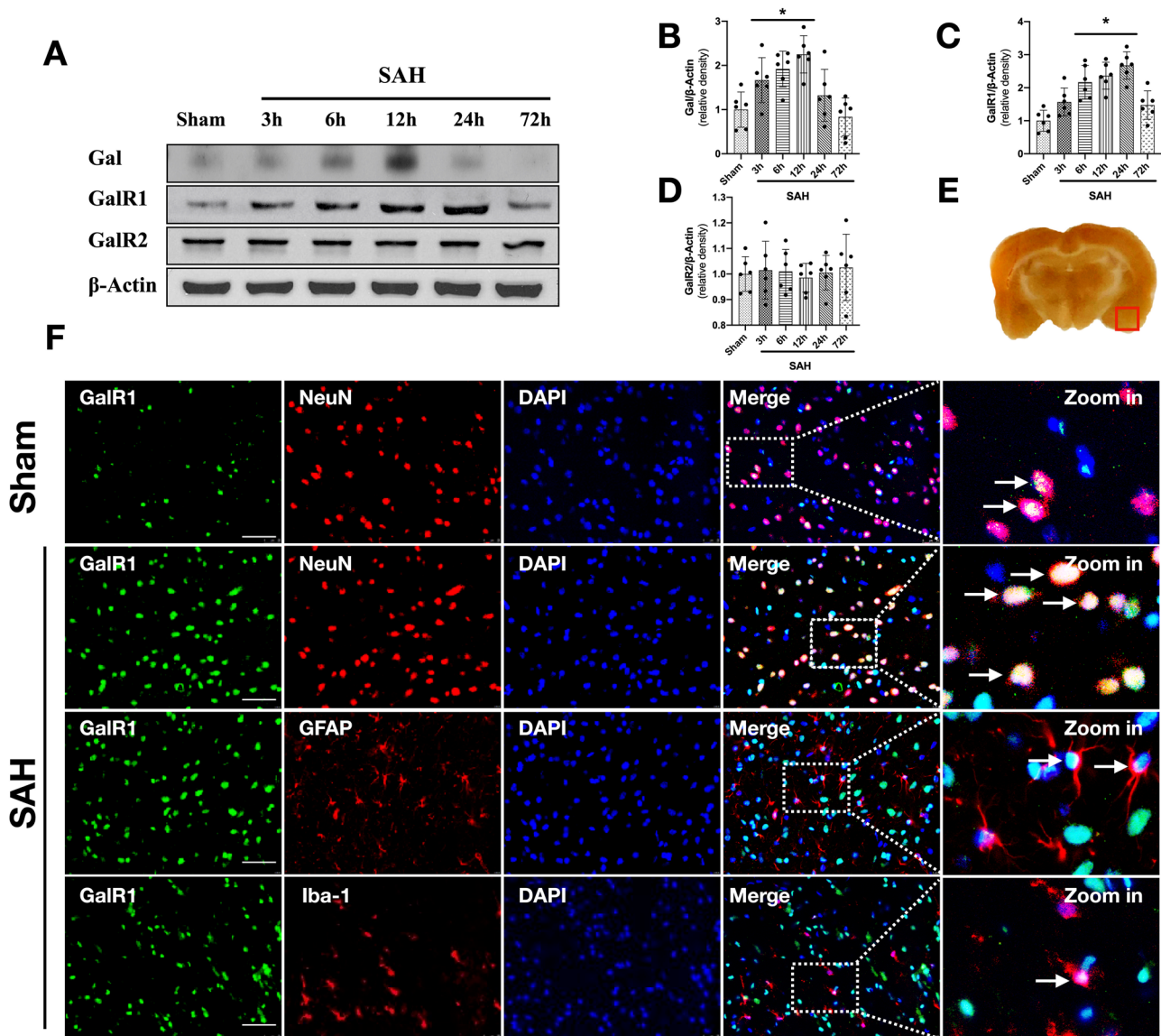


Fig. 2 Time course of Galanin (Gal), GalR1, GalR2, and cellular colocalization of GalR1 in brain after SAH. Representative western blot bands of time course (A) and densitometric quantification of Gal (B), GalR1 (C), and GalR2 (D) after SAH. * $P < 0.05$ vs. Sham group, Data was represented as mean \pm SD, $n = 6$ per group, one-way ANOVA, Tukey's post hoc test. (E) The small square shows the loca-

tion of the microphotograph. (F) Representative microphotographs of co-immunofluorescence staining of GalR1 (green) with neurons (NeuN, red), astrocytes (GFAP, green), and microglia (Iba-1, green) in the ipsilateral entorhinal cortex at 24 h after SAH. The Nuclei were stained with DAPI (blue). Arrows indicated the GalR1 positive cells. $n = 2$ per group

increased after GalR1 knockdown compared to SAH or SAH + Scr CRISPR group ($P < 0.05$; Fig. 3A, D, E). In addition, there was a significant decrease in Bcl-2 expression after SAH, which was further reduced by GalR1 knockdown (Fig. 3A, C) However, GalR2 knockdown did not statistically alter the protein levels of P53, Bcl-2, and Bax when compared with SAH or SAH + Scr CRISPR group ($P > 0.05$; Fig. 3).

GalR1 Knockdown Increased Neuronal Apoptosis and Neuronal Degeneration at 24 h After SAH

TUNEL staining and Fluoro-Jade C staining were performed to assess neuronal apoptosis and neuronal degeneration in the ipsilateral basal cortex at 24 h after SAH. The TUNEL-positive neurons and FJC-positive neurons were significantly increased after SAH, and further increased in GalR1 knockdown group

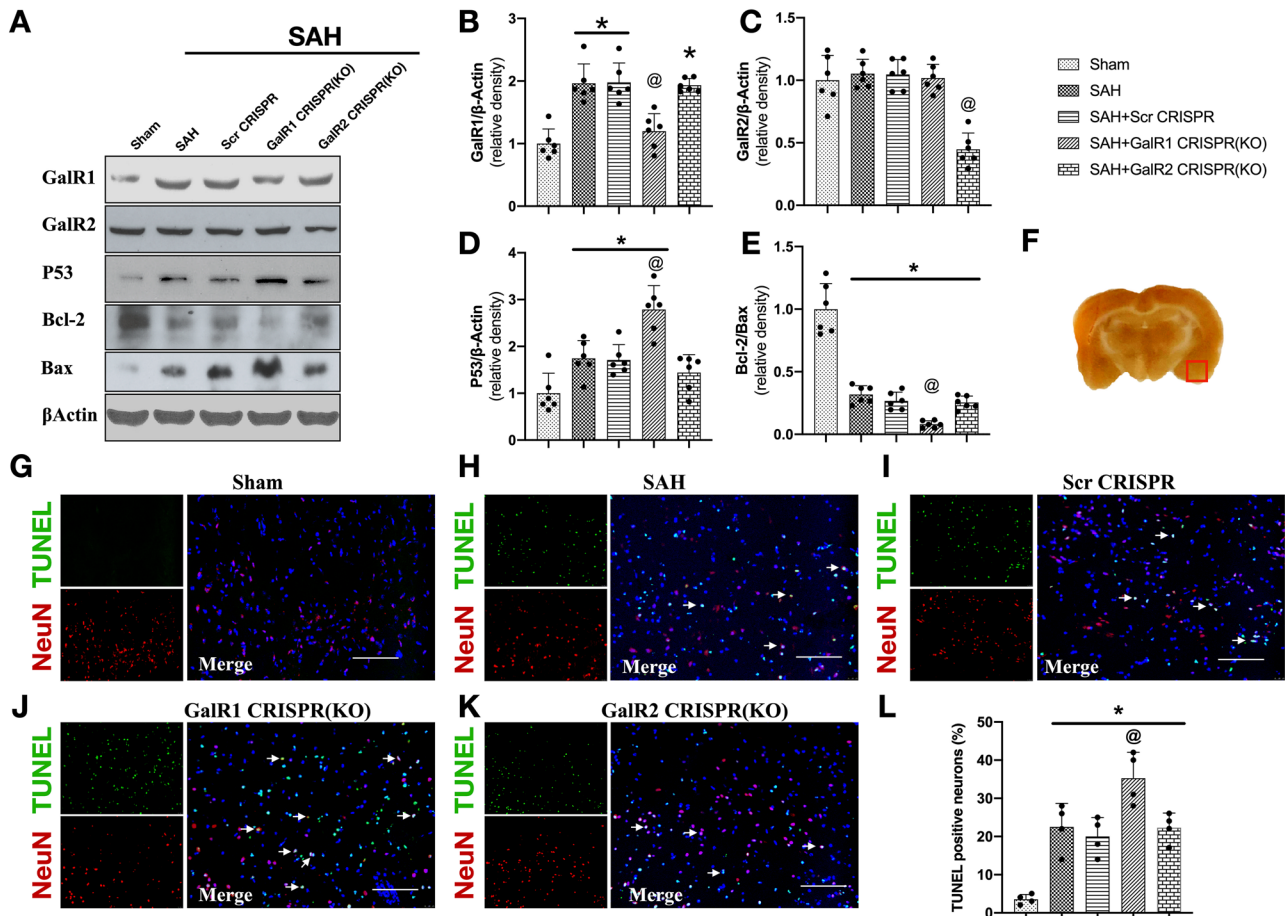


Fig. 3 GalR1 CRISPR knockdown increased expressions of apoptosis-related proteins and neuronal apoptosis at 24 h after SAH. Representative Western blots band (A) and densitometric quantification of GalR1 (B), GalR2 (C), P53 (D), and Bcl-2/Bax (E) after SAH. (F) The small square shows the location of the microphotograph. (G–L)

Representative micrographs and quantitative analysis of TUNEL-positive neurons in the ipsilateral entorhinal cortex at 24 h after SAH. Arrows indicated the apoptotic neurons. $n = 6$ per group. $*P < 0.05$ vs. Sham group, @ $P < 0.05$ vs. SAH + Scr CRISPR group

compared with sham, SAH, SAH + Scr CRISPR, and SAH + GalR2 CRISPR (KO) group (Figs. 3G–L and 4A, B).

GalR1 Knockdown Exacerbated Neurological Deficits at 24 h After SAH

At 24 h after SAH, both Modified Garcia scale and Beam Balance test showed significant neurological impairments in SAH, SAH + Scr CRISPR, and SAH + GalR1 CRISPR(KO), and SAH + GalR2 CRISPR(KO) groups when compared with Sham group ($P < 0.05$; Fig. 4C, D). CRISPR knockdown of GalR1, but not GalR2, exacerbated neurological deficits when compared with SAH or SAH + Scr CRISPR group ($P < 0.05$; Fig. 4C, D).

Activation of GalR1 Induced by M617 Improved Short-term Neurological Deficits at 24 h After SAH

The Modified Garcia score and Beam Balance test results demonstrated that neurological function was significantly impaired in rats in the SAH + PBS group compared with Sham group ($P < 0.05$; Fig. 5A, B). The medium dose (24 $\mu\text{g}/\text{kg}$) of M617 significantly improved neurological function, and the low (8 $\mu\text{g}/\text{kg}$) and high doses (72 $\mu\text{g}/\text{kg}$) of M617 only improved the modified Garcia score, but not the Beam Balance test scores ($P < 0.05$; Fig. 5A, B). Based on the neurological outcomes, we selected the medium dosage of 24 $\mu\text{g}/\text{kg}$ of M617 for the following experiments.

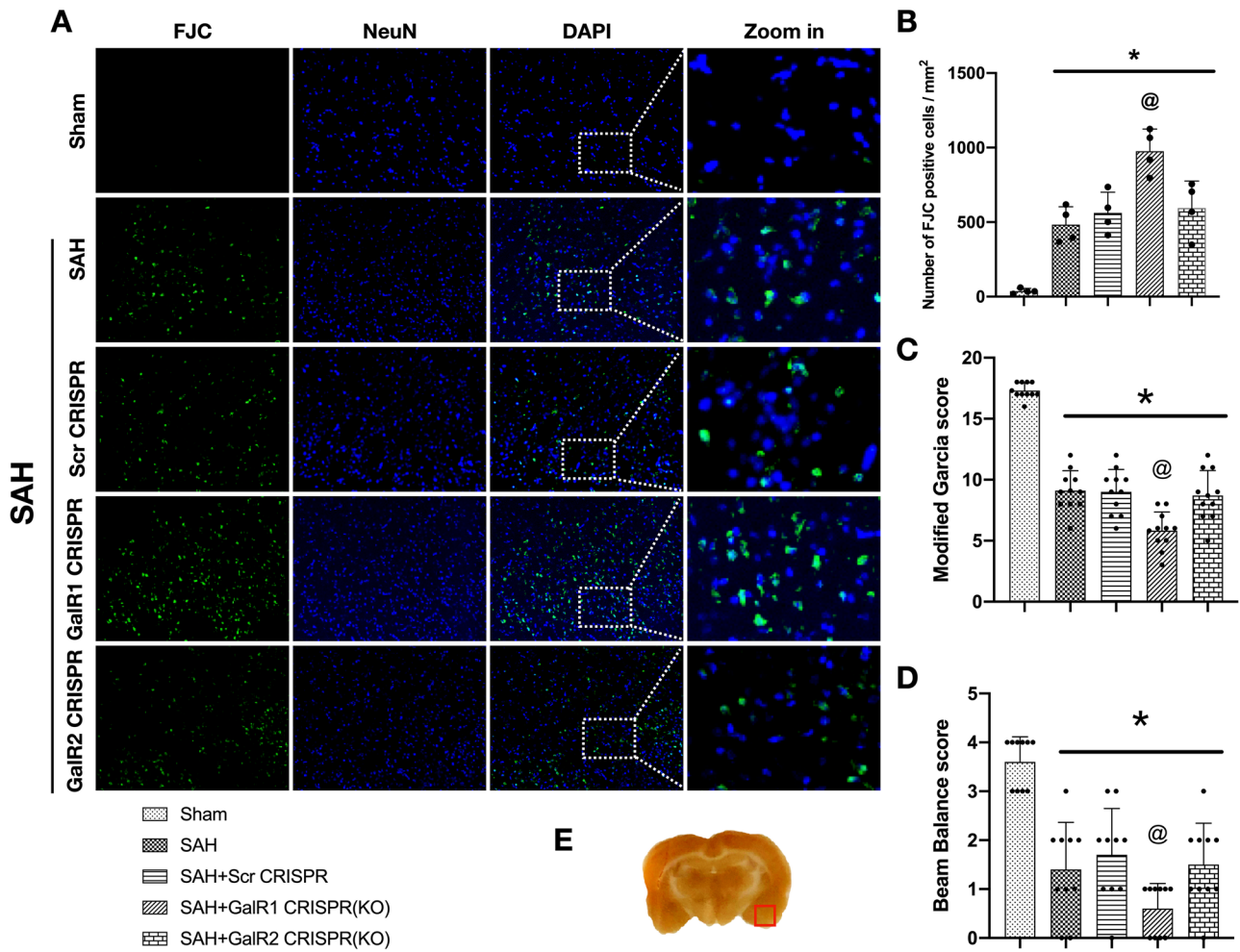


Fig. 4 GalR1 CRISPR knockdown exacerbated neurological deficits and increased neuronal degeneration at 24 h after SAH. Modified Garcia score (C) and Beam Balance score (D) in each group. *n* = 10 per group. (A–B) Representative microphotographs and quantitative

analysis of Fluoro-Jade C-positive neurons and TUNEL-positive neurons in the ipsilateral entorhinal cortex at 24 h after SAH. *n* = 5 per group. **P* < 0.05 vs. Sham group, @*P* < 0.05 vs. Scr CRISPR group

Activation of GalR1 Induced by M617 Reduced Neuronal Apoptosis and Neuronal Degeneration at 24 h After SAH

In the SAH + PBS group and SAH + PBS (3 h) group, TUNEL-positive or FJC-positive neurons were significantly increased at 24 h after SAH compared with the Sham group (*P* < 0.05; Fig. 5C–J). The activation of Gal with M617, at either 1 h or 3 h after SAH, consistently decreased the TUNEL-positive and Fluoro-Jade C positive neurons compared to PBS-treated SAH rats. (both *P* < 0.05; Fig. 5C–J).

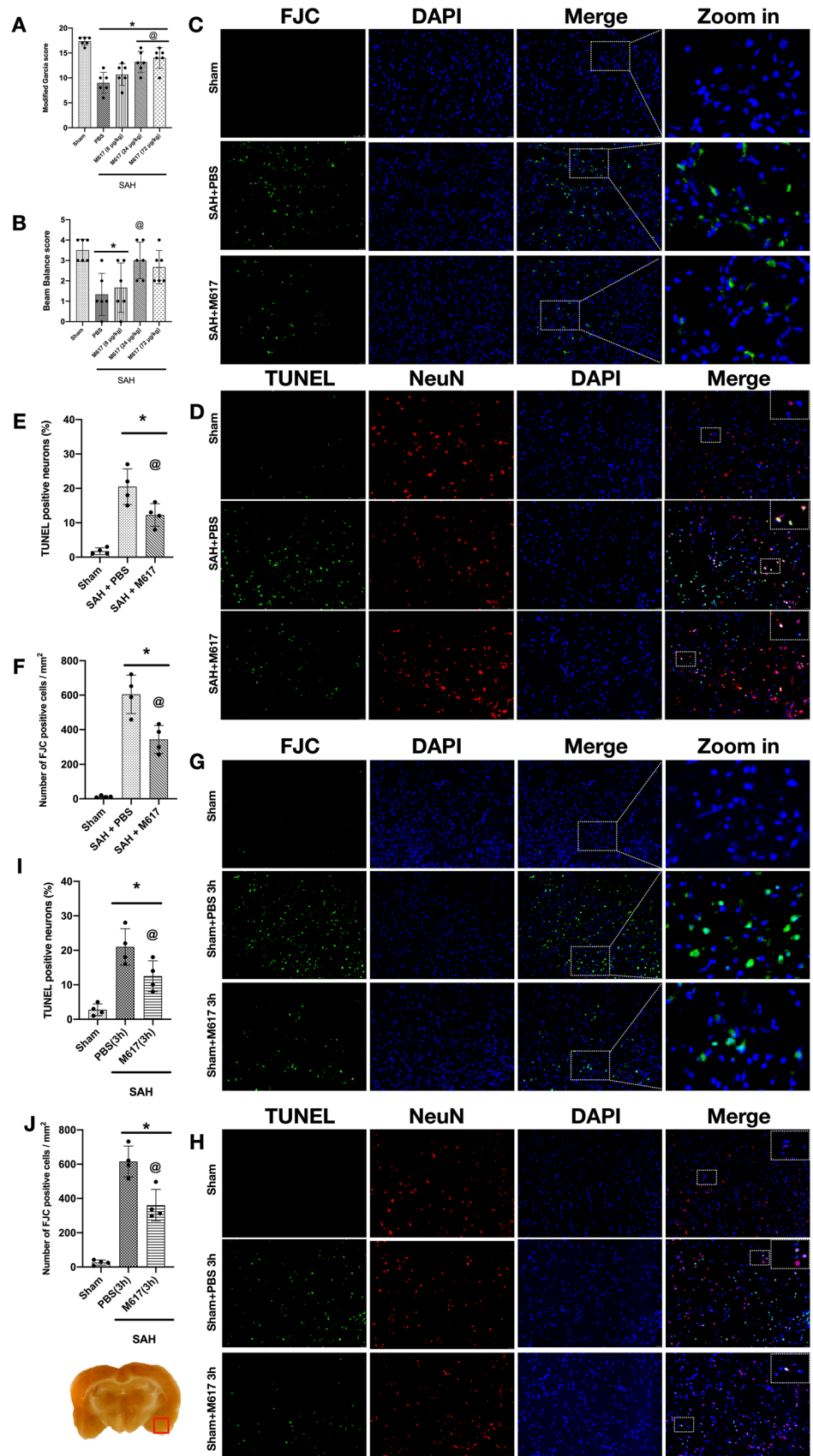
Activation of GalR1 Induced by M617 Improved Long-term Neurobehavioral Function After SAH

Rotarod test was performed to evaluate motor coordination after SAH on days 7, 14, and 21. Falling latency of rats

in SAH group was significantly decreased compared to the sham group (*P* < 0.05; Fig. 6A). M617 treatment significantly increased falling latency compared with SAH group on days 7 and 14, but on day 21 (*P* < 0.05), whereas no significant difference was observed between the SAH + M617 and SAH + PBS groups (*P* > 0.05; Fig. 6A).

The Morris water maze test, used to assess spatial learning and memory, demonstrated longer escape time, further swimming distance, and less time spent in the probe quadrant in the SAH + PBS group compared with sham group (Fig. 6C, D). The memory and learning abilities of the SAH + M617 treatment group improved significantly, as evidenced by their quicker escape times, closer escape routes, and extended time in target quadrant compared with sham group (both *P* < 0.05; Fig. 6C, D). There was no significant difference in swimming speed between the groups (both *P* > 0.05; Fig. 6E). The body weight of the rats among the groups

Fig. 5 Activation of GalR1 induced by M617 improved short-term neurological deficits and reduced neuronal apoptosis and neuronal degeneration at 24 h after SAH. M617 improved the Modified Garcia score (A) and Beam Balance score (B) at 24 h after SAH. (C–J) Representative microphotographs and quantitative analysis of Fluoro-Jade C positive neurons and TUNEL-positive neurons were performed at the ipsilateral basal cortex at 24 h after SAH. Vehicle: PBS. *n* = 4 per group. **P* < 0.05 vs. Sham group; @*P* < 0.0 vs. SAH + PBS group. Scale bar = 100 μm



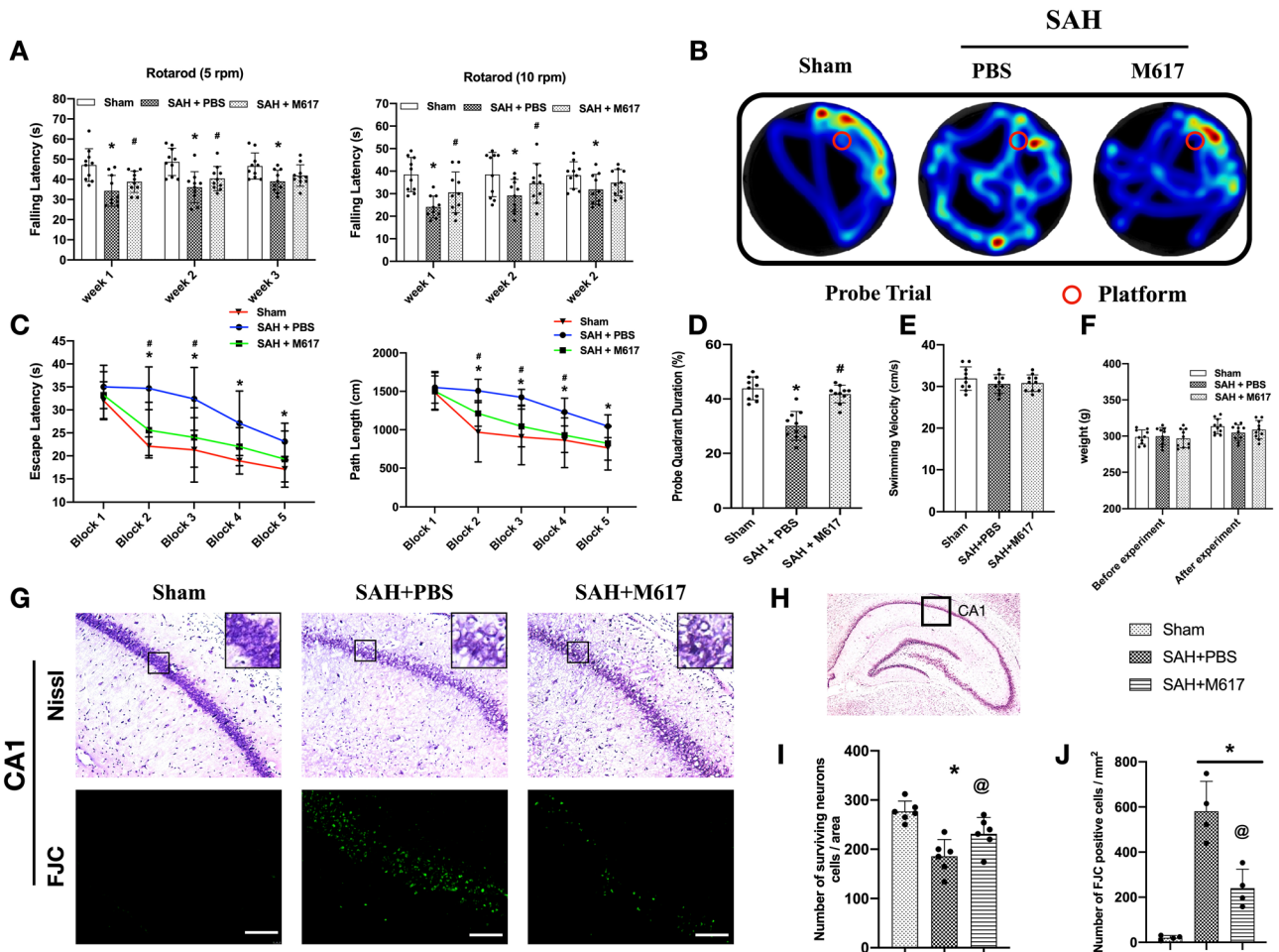


Fig. 6 Activation of GalR1 with M617 improved long-term neurobehavioral function, and reduced hippocampal neuronal degeneration at 28 days after SAH. (A) M617 increased falling latency in Rotarod test on days 7, 14, and 21 after SAH. (B) Representative thermal imaging of the probe trial. The red circles indicated the positions of the probe platform. (C) Escape latency and swimming distance of Morris water maze test on days 23–27 after SAH. (D) Quantification of the probe quadrant duration in the probe trial on day 27 after SAH. (E) Swimming velocities of different groups in probe trial. (F) Body weights

of each group before and after SAH. *n* = 10 per group. (G) Representative Nissl staining and Fluoro-Jade C staining microphotographs in Cornu Ammonis 1 (CA1) area of the hippocampus. Scale bar = 100µm. (H) The small square shows the area of interest for microphotograph. (I, J) Quantification of the surviving neurons and Fluoro-Jade C-positive neurons in CA1 at 28 days after modeling. *n* = 10 per group for neurobehavioral function, *n* = 6 per group for Nissl staining, and *n* = 4 per group for Fluoro-Jade C staining. *p***P* < 0.05 vs. Sham group; &*P* < 0.05 vs. SAH + PBS group

had no significant difference before (baseline) and after the treatment (*P* > 0.05; Fig. 6F).

decreased in SAH + M617 group when compared with SAH + PBS group (*P* < 0.05; Fig. 6G, I, J).

Activation of GalR1 with M617 Reduced Hippocampal Neuronal Degeneration at 28 days After SAH

Activation of GalR1 Induced by M617 Attenuated Neuronal Apoptosis via ERK/p GSK-3β/TIP60 Signaling Pathway at 24 h After SAH

Nissl staining and Fluoro-Jade staining were performed to detect degeneration of hippocampal neurons at 28 days after SAH. The CA1 region of the hippocampus in the SAH + PBS group had significant neuronal loss and degeneration compared to the sham group (*P* < 0.05; Fig. 6G, I, J). Surviving neurons in the hippocampal CA1 region were significantly increased, but degenerated neurons were significantly

While SAH significantly increased the expression of GalR1, pTIP60, p53, cleaved Caspase-3, and Bax at 24 h after SAH compared to sham group (*P* < 0.05; Fig. 7A, B), the expressions of pERK, pGSK-3β, and Bcl-2 remarkably decreased at 24 h after SAH compared to sham group. GalR1 activation induced by M617 increased the expression levels of GalR1, pERK, pGSK-3β, and Bcl-2 compared to the SAH + PBS

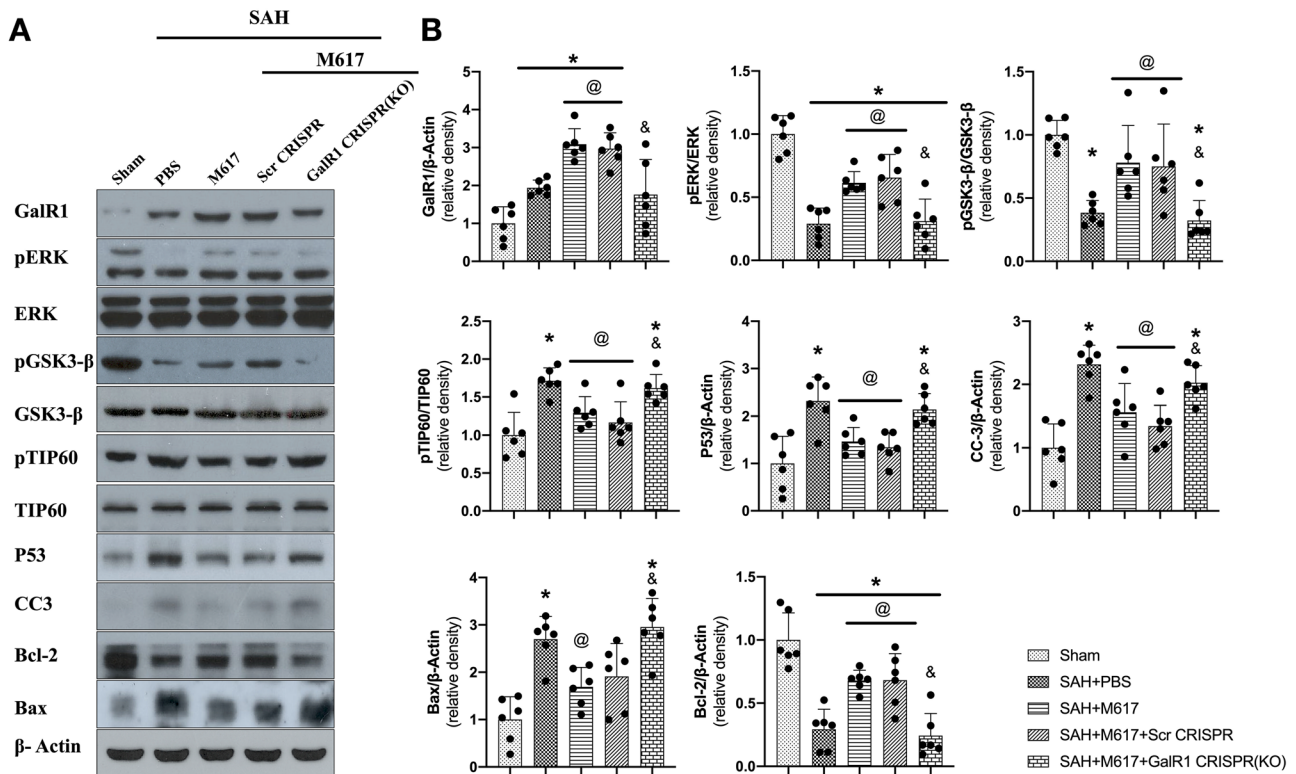


Fig. 7 GalR1 CRISPR knockdown abolished the anti-apoptotic effects of M617 at 24 h after SAH. GalR1 CRISPR knockdown abolished the anti-apoptotic effects of M617 at 24 h after SAH. Representative western blot bands (**A**) and densitometric quantification (**B**)

of GalR1, pERK, ERK, pGSK-3 β , GSK-3 β , pTIP60, TIP60, P53, CC3, Bcl-2, and Bax at 24 h after SAH. $n = 6$ per group. * $P < 0.05$ vs sham group; @ $P < 0.05$ vs SAH + PBS group; & $P < 0.05$ vs SAH + M617 + Scr CRISPR group

group ($P < 0.05$). Meanwhile, the expressions of pTIP60, p53, cleaved Caspase-3, and Bax were decreased in the SAH + M617 group compared with the SAH + PBS group ($P < 0.05$; Fig. 7A–B).

GalR1 knockdown by GalR1 CRISPR pretreatment significantly decreased the downstream protein levels, such as pERK, pGSK-3 β , and Bcl-2, in the SAH + M617 + GalR1 CRISPR group compared with those in the SAH + M617 + scrambled CRISPR group ($P < 0.05$; Fig. 7A–B). Significantly higher expression levels of pTIP60, p53, Bax, and Caspase-3 were consistently observed in the SAH + M617 + GalR1 CRISPR group than in the SAH + M617 + scrambled CRISPR group ($P < 0.05$; Fig. 7A, B).

Pretreatment with ERK inhibitor, U0126, significantly suppressed the expression of pERK, pGSK-3 β , and Bcl-2, but increased the protein levels of pTIP60, p53, cleaved Caspase-3, and Bax in the SAH + M617 + U0126 group compared with the SAH + M617 + DMSO group ($P < 0.05$; Fig. 8A, B). Additionally, pretreatment with GSK-3 β activation CRISPR significantly increased protein levels of GSK-3 β , pTIP60, p53, cleaved Caspase-3, and Bax, but suppressed the expression of Bcl-2 at 24 h after SAH in the

SAH + M617 + GSK-3 β CRISPR (ACT.) group compared with the SAH + M617 + Scr CRISPR group (Fig. 8C, D).

Discussion

Subarachnoid hemorrhage is a devastating cerebrovascular disease without an effective treatment [7]. Delayed vasospasm occurs after subarachnoid hemorrhage, leading to a poor prognosis for the patient [41]. However, early brain injury precedes delayed cerebral vasospasm after the onset of SAH [42]. Early brain injury involves signaling pathways of neuronal apoptosis, inflammation, and oxidative stress response [43]. A plethora of studies have demonstrated that therapeutic intervention against neuronal apoptosis can alleviate early brain injury and improve neurological deficits after SAH [6, 8, 44, 45]. This present study is the first to evaluate the neuroprotective function of GalR1 activation induced by M617, and we have explored its anti-apoptotic mechanisms in the acute phase of a rat model of SAH. The main novel findings of this study are as follows: (1) Endogenous protein levels of galanin and its receptor, GalR1,

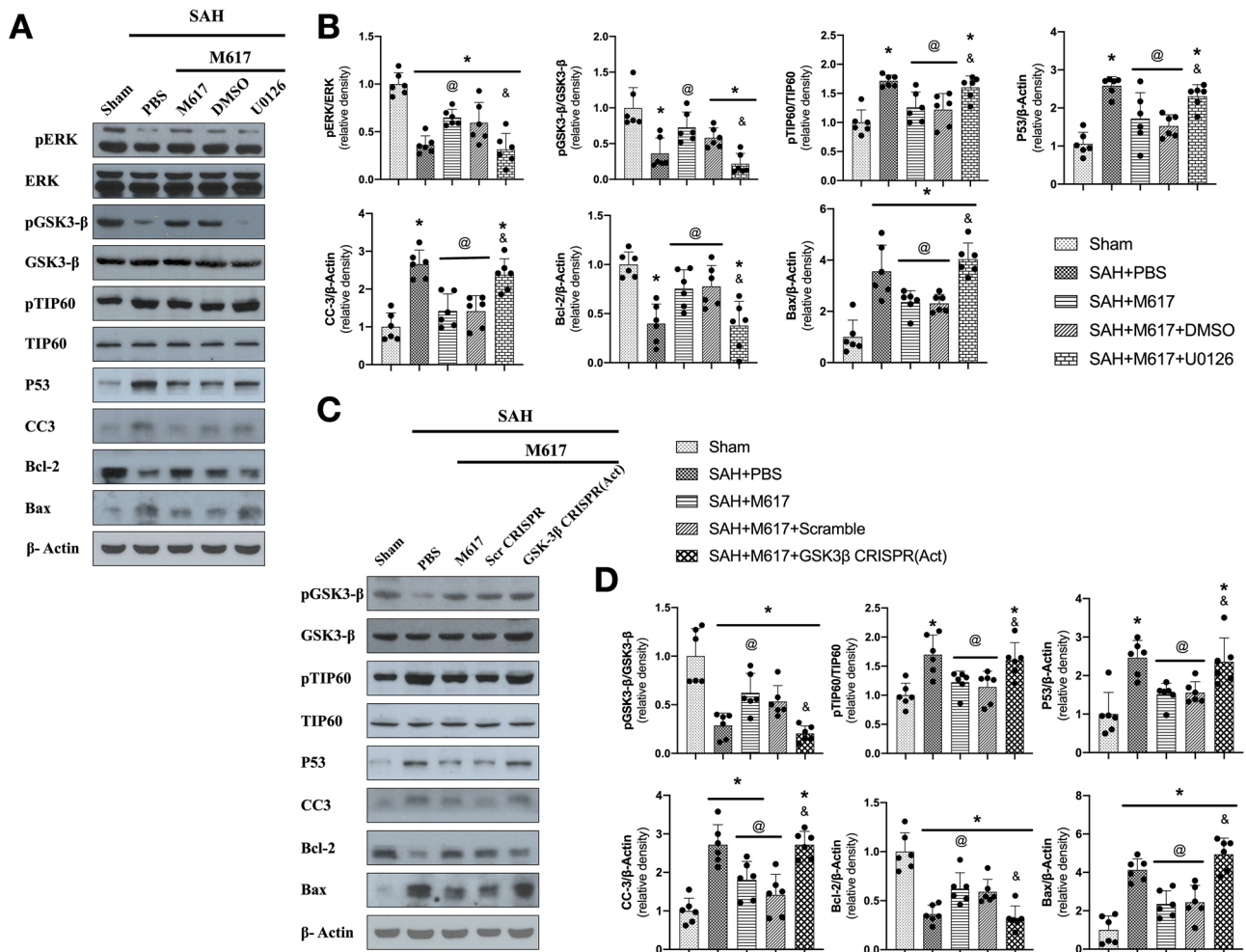


Fig. 8 ERK inhibitor U0126 and GSK-3 β CRISPR activation abolished anti-apoptotic effects of M617 at 24 h after SAH. Representative western blot bands (A, C) and densitometric quantification (B, D) of pERK, ERK, pGSK3- β , GSK3- β , pTIP60, TIP60, P53, CC3, Bcl-

2, and Bax at 24 h after SAH. $n = 6$ per group. * $P < 0.05$ vs sham group; @ $P < 0.05$ vs SAH + PBS group; & $P < 0.05$ vs SAH + M17 + Scr CRISPR group

were increased in the ipsilateral brain, and peaked at 12 h and 24 h, respectively, after SAH. GalR1 was expressed on neurons, astrocytes, and microglia at 24 h after SAH; (2) CRISPR knockdown of GalR1, but not GalR2, exacerbated neurological deficits and neuronal apoptosis at 24 h after SAH; (3) activation of GalR1 with M617 at a dose of 24 μ g/kg not only significantly improved short- and long-term neurological deficits, but also decreased neuronal apoptosis and degeneration in the ipsilateral temporal cortex and hippocampus; (4) activation of GalR1 induced by M617 upregulated the protein levels of pERK, pGSK3- β , and Bcl-2, but downregulated the protein levels of pTIP60, P53, cleaved caspase-3, and Bax in the ipsilateral hemisphere at 24 h after SAH; (5) CRISPR knockdown of GalR1, inhibition of ERK, or activation of GSK-3 β abolished the beneficial effects of M617 on neurological deficits and expressions of apoptosis-related proteins at 24 h after SAH. Taken together, our data

suggests that GalR1 activation induced by M617 attenuates neuronal apoptosis and that the neuroprotective effect is exerted, at least partially, through the ERK/p GSK-3 β /TIP60 signaling pathway after SAH in rats.

As a neuropeptide, the expression level of galanin was elevated with the resultant functionalities in many diseases, such as brain trauma, ischemia, mood disorder, tumor, drug addiction, and Alzheimer's disease [17, 19, 46, 47]. Consistently, we also observed the elevation of galanin after SAH in rats. The various effects of galanin act through three subtypes of galanin receptors, namely, GalR1, GalR2, and GalR3. GalR1 mRNA, and GalR2 mRNA are broadly expressed in the mammalian CNS, but GalR3 mRNA is relatively abundant in peripheral tissues, and only has restricted expression in the hypothalamus, midbrain, and hindbrain of CNS [48, 49]. GalR1 activation exerts different effects than that of GalR2. Previous studies have demonstrated that

activation of GalR1 or inhibition of GalR2 has antidepressant effects [50]. GalR1 activation inhibits cell proliferation, and GalR2 activation promotes apoptosis in head and neck squamous cell carcinoma [18, 51]. In contrast to the proapoptotic effect of GalR2 in head and neck squamous cell carcinoma [15], silencing of GalR1 and its ligand, galanin, has been shown to induce apoptosis in the colorectal cancer cell line [16]. GalR2 activation inhibited shear stress-induced nerve damage in cultured cortical neurons in rats [17, 52], and had antioxidant effects in cortical astrocytes [53]. In an ischemic stroke mouse model, galanin reduced infarct size and improved neurological deficits via GalR1 activation [17]. In the present study, there were no significant changes of GalR2, which coincided with the results found in an *in vitro* model of high glucose-induced dorsal root ganglion (DRG) neuronal death, in which GalR2 expression was also not significantly altered [12]. The remarkable upregulation of GalR1 accompanied the increased galanin over time after SAH, suggesting the likelihood of galanin-mediated GalR1 activation as an endogenous neuroprotective mechanism in the setting of SAH.

In a healthy brain, GalR1 mRNA is widely expressed in neurons, but is minimally expressed in astrocytes, and rarely expressed in microglia [13, 54]. GalR1 is distributed predominantly in olfactory structures and subregions/nuclei of the amygdala, thalamus, hypothalamus, pons, medulla, and spinal cord [55, 56]. Anatomical studies have identified GalR1 and GalR2 mRNA in cells within the subventricular zone and the rostral migratory stream, regions associated with neurogenesis in the adult brain [57]. In a mouse cerebral ischemia model, GalR1 was found to be extensively present in neurons of the cerebral cortex, and was associated with neuronal apoptosis [17]. We further validated the significance of GalR1 in SAH using GalR1 and GalR2 knockdown CRISPR, respectively. The CRISPR knockdown of GalR1, but not GalR2, exacerbated neurological deficits, and further increased neuronal apoptosis and degeneration at 24 h after SAH compared with the scramble CRISPR group. There were higher expression levels of pro-apoptotic Bax, but lower anti-apoptotic Bcl-2 protein levels in ipsilateral brain tissues in GalR1 knockdown SAH rats. Similarly, GalR1 knockdown caused severe hippocampal neuron loss in a mouse model of epilepsy [58]. These results confirm the time course finding regarding GalR1 involvement in the endogenous neuroprotective mechanism of galanin after SAH.

Due to the concern of inconsistent effects exerted by galanin via GalR1 and GalR2 activation, we evaluated the therapeutic effects of selective activation of GalR1 induced by exogenous M617 in the present study. Intranasal M617 administration at 1 h after SAH significantly improved short-term neurological deficits, long-term spatial memory, and learning function compared with vehicle-treated SAH rats.

The integrity of hippocampal neurons impaired spatial memory and learning functions, and further impaired the cognitive functions in rats [59, 60]. There was significant neuronal degeneration in CA1 of the hippocampus at 28 days after SAH in rats. The neurological benefits of selective GalR1 activation induced by M617 were associated with significantly less neuronal apoptosis and degeneration in ipsilateral hemisphere, as assessed by TUNEL staining and FJC staining. The western blots assay consistently demonstrated that M617 treatment significantly down-regulated the proapoptotic protein levels of Bax and cleaved Caspase-3, but up-regulated anti-apoptotic Bcl-2 within the ipsilateral brain tissues at 24 h after SAH.

It was noted that intranasal administration of M617 at 3 h after SAH, a clinically relevant time window, provided comparable neuroprotection to that of early delivery at 1 h after SAH, suggesting its potential translational value in treating SAH patients. Although intracerebroventricular administration of M617 reportedly increased the body weight of type 2 diabetic rats by decreasing skeletal muscle insulin resistance [61], we did not observe significant changes in body weight associated with the dosage of the single-dose treatment regimen of M617 in the present SAH model.

We further explored the signaling pathway underlying the anti-apoptotic effects of GalR1 activation induced by M617. GalR1 activation has been shown to promote phosphorylation of ERK, subsequently inhibiting squamous tumor cell proliferation [60]. GSK-3 β (Ser9) phosphorylation is a downstream target of pERK [62, 63], and the pro-apoptotic effect of GSK-3 β could be inhibited by phosphorylation at ser9 [64]. GSK-3 β phosphorylated TIP60 on Ser86, which promotes p53-mediated apoptosis by inducing antiapoptotic BCL-2 family member, PUMA [65–67]. In the present study, we found that the expression level of phosphorylated ERK (pERK), pGSK-3 β , and Bcl-2 were significantly increased following M617-mediated activation of GalR1 in the ipsilateral brain hemisphere at 24 h after SAH. The effects of M617 on the phosphorylation of ERK and GSK-3 β were reversed by CRISPR knockdown of GalR1, as well as by U0126, an inhibitor of ERK. GSK-3 β activation CRISPR has no effects on upstream pERK levels, but reduced pGSK-3 β . All of the interventions abolished the suppression effects of M617 on expressions of pTIP60, as well as apoptosis-related proteins, including P53, cleaved caspase-3, and Bax at 24 h after SAH. Our data suggested that the anti-neuronal apoptotic effects of M617-mediated GalR1 activation acted, at least in part, via ERK/GSK-3 β /TIP60 signaling pathway.

Delayed vasospasm occurs after subarachnoid hemorrhage, leading to a poor prognosis for the patient [41]. However, a growing number of studies have found that early brain injury precedes delayed cerebral vasospasm after the onset of subarachnoid hemorrhage [42]. Early brain injury involves signaling pathways of neuronal apoptosis,

inflammation, oxidative stress response, anti-neuronal apoptosis, and protection of neurovascular units that are effective early brain injury treatments [43, 45]. In this study, M617 treatment attenuated neuronal apoptosis 24 h, demonstrating the neuroprotective effects against acute neural injury after SAH.

There are several limitations in this study. First, the optimal therapeutic regimen of M617 treatment for SAH was not evaluated in the present study. Second, GalR1 is expressed not only in neurons, but also in microglia and astrocytes. We cannot exclude that the neuroprotective effects exerted by GalR1 activation may involve these two brain cell types after SAH. Third, we are focusing on ERK/GSK-3 β /TIP60 signaling, but other mechanisms underlying the anti-apoptotic effects of GalR1 activation require further investigation.

Conclusion

In conclusion, M617-mediated activation of GalR1 improved neurological function by reducing neuronal apoptosis after SAH in rats. The anti-apoptotic effect acted, at least partially, through the ERK/GSK-3 β /TIP60 signaling pathway. GalR1 may serve as a promising therapeutic target for patients with SAH.

Supplementary Information The online version contains supplementary material available at <https://doi.org/10.1007/s13311-021-01066-x>.

Required Author Forms Disclosure forms provided by the authors are available with the online version of this article.

Funding This study was supported by grants from the National Institutes of Health (NS081740 and NS082184) of John H. Zhang.

Declarations

Ethics Approval and Consent to Participate All animal experiments were approved by the Institutional Animal Care and Use Committee at Loma Linda University. The study followed the Health's Guide for the Care and Use of Laboratory Animals (National Research Council) and complied with the ARRIVE guidelines for reporting in vivo experiments.

Conflict of Interest The authors declare no competing interests.

References

- Petridis AK, Kamp MA, Cornelius JF *et al*. Aneurysmal Subarachnoid Hemorrhage. *Dtsch Arztebl Int*, 114(13), 226-236 (2017).
- Korja M, Kaprio J. Controversies in epidemiology of intracranial aneurysms and SAH. *Nat Rev Neurol*, 12(1), 50-55 (2016).
- Takemoto Y, Hasegawa Y, Hayashi K *et al*. The Stabilization of Central Sympathetic Nerve Activation by Renal Denervation Prevents Cerebral Vasospasm after Subarachnoid Hemorrhage in Rats. *Transl Stroke Res*, 11(3), 528-540 (2020).
- Ostrowski RP, Colohan AR, Zhang JH. Molecular mechanisms of early brain injury after subarachnoid hemorrhage. *Neurological Research*, 28(4), 399-414 (2006).
- Rass V, Helbok R. Early Brain Injury After Poor-Grade Subarachnoid Hemorrhage. *Curr Neurol Neurosci Rep*, 19(10), 78 (2019).
- Mo J, Enkhjargal B, Travis ZD *et al*. AVE 0991 attenuates oxidative stress and neuronal apoptosis via Mas/PKA/CREB/UCP-2 pathway after subarachnoid hemorrhage in rats. *Redox Biol*, 20, 75-86 (2019).
- Cahill J, Cahill WJ, Calvert JW, Calvert JH, Zhang JH. Mechanisms of early brain injury after subarachnoid hemorrhage. *J Cereb Blood Flow Metab*, 26(11), 1341-1353 (2006).
- Luo X, Li L, Xu W, Cheng Y, Xie Z. HLY78 Attenuates Neuronal Apoptosis via the LRP6/GSK3 β -Catenin Signaling Pathway After Subarachnoid Hemorrhage in Rats. *Neurosci Bull*, (2020).
- Šípková J, Kramáriková I, Hynie S, Klenerová V. The galanin and galanin receptor subtypes, its regulatory role in the biological and pathological functions. *Physiol Res*, 66(5), 729-740 (2017).
- Kask K, Berthold M, Bartfai T. Galanin receptors: involvement in feeding, pain, depression and Alzheimer's disease. *Life Sci*, 60(18), 1523-1533 (1997).
- Zachariou V, Brunzell DH, Hawes J *et al*. The neuropeptide galanin modulates behavioral and neurochemical signs of opiate withdrawal. *Proc Natl Acad Sci USA*, 100(15), 9028-9033 (2003).
- Xu X, Jiang H, Liu H, Zhang W, Xu X, Li Z. The effects of galanin on dorsal root ganglion neurons with high glucose treatment in vitro. *Brain Res Bull*, 87(1), 85-93 (2012).
- Lang R, Gundlach AL, Kofler B. The galanin peptide family: receptor pharmacology, pleiotropic biological actions, and implications in health and disease. *Pharmacol Ther*, 115(2), 177-207 (2007).
- Kanazawa T, Iwashita T, Kommareddi P *et al*. Galanin and galanin receptor type 1 suppress proliferation in squamous carcinoma cells: activation of the extracellular signal regulated kinase pathway and induction of cyclin-dependent kinase inhibitors. *Oncogene*, 26(39), 5762-5771 (2007).
- Uehara T, Kanazawa T, Mizukami H *et al*. Novel anti-tumor mechanism of galanin receptor type 2 in head and neck squamous cell carcinoma cells. *Cancer Sci*, 105(1), 72-80 (2014).
- Stevenson L, Allen WL, Turkington R *et al*. Identification of galanin and its receptor GalR1 as novel determinants of resistance to chemotherapy and potential biomarkers in colorectal cancer. *Clin Cancer Res*, 18(19), 5412-5426 (2012).
- Li Y, Mei Z, Liu S *et al*. Galanin Protects from Caspase-8/12-initiated Neuronal Apoptosis in the Ischemic Mouse Brain via GalR1. *Aging Dis*, 8(1), 85-100 (2017).
- Webbing K, Groves-Chapman JL, Runesson J *et al*. Pharmacological stimulation of GAL1R but not GAL2R attenuates kainic acid-induced neuronal cell death in the rat hippocampus. *Neuropeptides*, 58, 83-92 (2016).
- Lang R, Gundlach AL, Holmes FE *et al*. Physiology, signaling, and pharmacology of galanin peptides and receptors: three decades of emerging diversity. *Pharmacol Rev*, 67(1), 118-175 (2015).
- Ciftci E, Karacay R, Caglayan A *et al*. Neuroprotective effect of lithium in cold-induced traumatic brain injury in mice. *Behav Brain Res*, 392, 112719 (2020).
- Chiu C-T, Wang Z, Hunsberger JG, Chuang D-M. Therapeutic potential of mood stabilizers lithium and valproic acid: beyond bipolar disorder. *Pharmacological reviews*, 65(1), 105-142 (2013).
- Tang J, Hu Q, Chen Y *et al*. Neuroprotective role of an N-acetyl serotonin derivative via activation of tropomyosin-related kinase

- receptor B after subarachnoid hemorrhage in a rat model. *Neurobiol Dis*, 78, 126-133 (2015).
23. Ma J, Wang Z, Liu C *et al*. Pramipexole-Induced Hypothermia Reduces Early Brain Injury via PI3K/AKT/GSK3 β pathway in Subarachnoid Hemorrhage rats. *Scientific reports*, 6, 23817 (2016).
 24. Xu H, Li J, Wang Z *et al*. Methylene blue attenuates neuroinflammation after subarachnoid hemorrhage in rats through the Akt/GSK-3 β /MEF2D signaling pathway. *Brain Behav Immun*, 65, 125-139 (2017).
 25. Nie T, Yang S, Ma H *et al*. Regulation of ER stress-induced autophagy by GSK3 β -TIP60-ULK1 pathway. *Cell Death Dis*, 7(12), e2563 (2016).
 26. Wang P, Bao H, Zhang X-P, Liu F, Wang W. Regulation of Tip60-dependent p53 acetylation in cell fate decision. *FEBS letters*, 593(1), 13-22 (2019).
 27. Ghobashi AH, Kamel MA. Tip60: updates. *J Appl Genet*, 59(2), 161-168 (2018).
 28. Feng D, Wang B, Ma Y *et al*. The Ras/Raf/Erk Pathway Mediates the Subarachnoid Hemorrhage-Induced Apoptosis of Hippocampal Neurons Through Phosphorylation of p53. *Molecular neurobiology*, 53(8), 5737-5748 (2016).
 29. Parthasarathy G, Philipp MT. The MEK/ERK pathway is the primary conduit for Borrelia burgdorferi-induced inflammation and P53-mediated apoptosis in oligodendrocytes. *Apoptosis*, 19(1), 76-89 (2014).
 30. Enkhjargal B, McBride DW, Manaenko A *et al*. Intranasal administration of vitamin D attenuates blood-brain barrier disruption through endogenous upregulation of osteopontin and activation of CD44/P-gp glycosylation signaling after subarachnoid hemorrhage in rats. *J Cereb Blood Flow Metab*, 37(7), 2555-2566 (2017).
 31. Sugawara T, Ayer R, Jadhav V, Zhang JH. A new grading system evaluating bleeding scale in filament perforation subarachnoid hemorrhage rat model. *J Neurosci Methods*, 167(2), 327-334 (2008).
 32. Zhou K, Enkhjargal B, Xie Z *et al*. Dihydrolipoic Acid Inhibits Lysosomal Rupture and NLRP3 Through Lysosome-Associated Membrane Protein-1/Calcium/Calmodulin-Dependent Protein Kinase II/TAK1 Pathways After Subarachnoid Hemorrhage in Rat. *Stroke*, 49(1), 175-183 (2018).
 33. Hu X, Yan J, Huang L *et al*. INT-777 attenuates NLRP3-ASC inflammasome-mediated neuroinflammation via TGR5/cAMP/PKA signaling pathway after subarachnoid hemorrhage in rats. *Brain, behavior, and immunity*, 91, 587-600 (2021).
 34. Fumoto T, Naraoka M, Katagai T, Li Y, Shimamura N, Ohkuma H. The Role of Oxidative Stress in Microvascular Disturbances after Experimental Subarachnoid Hemorrhage. *Transl Stroke Res*, 10(6), 684-694 (2019).
 35. Pang J, Peng J, Matei N *et al*. Apolipoprotein E Exerts a Whole-Brain Protective Property by Promoting M1⁺ Microglia Quiescence After Experimental Subarachnoid Hemorrhage in Mice. *Transl Stroke Res*, 9(6), 654-668 (2018).
 36. Bromley-Brits K, Deng Y, Song W. Morris water maze test for learning and memory deficits in Alzheimer's disease model mice. *J Vis Exp*, (53) (2011).
 37. Gorlamandala N, Parmar J, Craig AJ *et al*. Focal Ischaemic Infarcts Expand Faster in Cerebellar Cortex than Cerebral Cortex in a Mouse Photothrombotic Stroke Model. *Transl Stroke Res*, 9(6), 643-653 (2018).
 38. Fang Y, Shi H, Ren R *et al*. Pituitary Adenylate Cyclase-Activating Polypeptide Attenuates Brain Edema by Protecting Blood-Brain Barrier and Glymphatic System After Subarachnoid Hemorrhage in Rats. *Neurotherapeutics*, (2020).
 39. Zuo G, Zhang T, Huang L *et al*. Activation of TGR5 with INT-777 attenuates oxidative stress and neuronal apoptosis via cAMP/PKCepsilon/ALDH2 pathway after subarachnoid hemorrhage in rats. *Free Radic Biol Med*, 143, 441-453 (2019).
 40. Mahmood T, Yang P-C. Western blot: technique, theory, and trouble shooting. *N Am J Med Sci*, 4(9), 429-434 (2012).
 41. Sobey C, Faraci F. Subarachnoid haemorrhage: what happens to the cerebral arteries? *Clinical and experimental pharmacology & physiology*, 25(11), 867-876 (1998).
 42. Fujii M, Yan J, Rolland W, Soejima Y, Caner B, Zhang J. Early brain injury, an evolving frontier in subarachnoid hemorrhage research. *Transl Stroke Res*, 4(4), 432-446 (2013).
 43. Cahill J, Zhang J. Subarachnoid hemorrhage: is it time for a new direction? *Stroke*, 40, S86-87 (2009).
 44. Sun C, Enkhjargal B, Reis C *et al*. Osteopontin-Enhanced Autophagy Attenuates Early Brain Injury via FAK-ERK Pathway and Improves Long-Term Outcome after Subarachnoid Hemorrhage in Rats. *Cells*, 8(9) (2019).
 45. Okada T, Enkhjargal B, Travis ZD *et al*. FGF-2 Attenuates Neuronal Apoptosis via FGFR3/PI3k/Akt Signaling Pathway After Subarachnoid Hemorrhage. *Mol Neurobiol*, 56(12), 8203-8219 (2019).
 46. Palkeeva M, Studneva I, Molokoedov A *et al*. Galanin/GalR1-3 system: A promising therapeutic target for myocardial ischemia/reperfusion injury. *Biomed Pharmacother*, 109, 1556-1562 (2019).
 47. Mei Z, Yang Y, Li Y *et al*. Galanin suppresses proliferation of human U251 and T98G glioma cells via its subtype 1 receptor. *Biol Chem*, 398(10), 1127-1139 (2017).
 48. Burazin TC, Larm JA, Ryan MC, Gundlach AL. Galanin-R1 and -R2 receptor mRNA expression during the development of rat brain suggests differential subtype involvement in synaptic transmission and plasticity. *Eur J Neurosci*, 12(8), 2901-2917 (2000).
 49. Mennicken F, Hoffert C, Pelletier M, Ahmad S, O'Donnell D. Restricted distribution of galanin receptor 3 (GalR3) mRNA in the adult rat central nervous system. *J Chem Neuroanat*, 24(4), 257-268 (2002).
 50. Kuteeva E, Hökfelt T, Wardi T, Ogren SO. Galanin, galanin receptor subtypes and depression-like behaviour. *Cellular and molecular life sciences : CMLS*, 65(12), 1854-1863 (2008).
 51. Li SY, Huo ML, Wu XY *et al*. Involvement of galanin and galanin receptor 1 in nociceptive modulation in the central nucleus of amygdala in normal and neuropathic rats. *Sci Rep*, 7(1), 15317 (2017).
 52. Liu M, Song W, Li P *et al*. Galanin protects against nerve injury after shear stress in primary cultured rat cortical neurons. *PLoS ONE*, 8(5), e63473 (2013).
 53. Sun J, Xu S, Li H, Li L, Xu ZD. Galanin Protects Rat Cortical Astrocyte from Oxidative Stress: Involvement of GalR2 and pERK1/2 Signal Pathway. *Mediators Inflamm*, 2019, 2716028 (2019).
 54. Shen P, Larm J, Gundlach A. Expression and plasticity of galanin systems in cortical neurons, oligodendrocyte progenitors and proliferative zones in normal brain and after spreading depression. *Eur J Neurosci*, 18(6), 1362-1376 (2003).
 55. Hohmann JG, Juréus A, Teklemichael DN, Matsumoto AM, Clifton DK, Steiner RA. Distribution and regulation of galanin receptor 1 messenger RNA in the forebrain of wild type and galanin-transgenic mice. *Neuroscience*, 117(1), 105-117 (2003).
 56. O'Donnell D, Ahmad S, Wahlestedt C, Walker P. Expression of the novel galanin receptor subtype GALR2 in the adult rat CNS: Distinct distribution from GALR1. *Journal of Comparative Neurology*, 409(3), 469-481 (1999).
 57. Mazarati A, Lu X, Shinmei S, Badie-Mahdavi H, Bartfai T. Patterns of seizures, hippocampal injury and neurogenesis in three models of status epilepticus in galanin receptor type 1 (GalR1) knockout mice. *Neuroscience*, 128(2), 431-441 (2004).
 58. Schauwecker PE. Galanin receptor 1 deletion exacerbates hippocampal neuronal loss after systemic kainate administration in mice. *PLoS ONE*, 5(12), e15657 (2010).

59. Neiva R, Caulino-Rocha A, Ferreirinha F, Lobo MG, Correia-de-Sá P. Non-genomic Actions of Methylprednisolone Differentially Influence GABA and Glutamate Release From Isolated Nerve Terminals of the Rat Hippocampus. *Front Mol Neurosci*, 13, 146 (2020).
60. Alkhunizi SM, Fakhoury M, Abou-Kheir W, Lawand N. Gadolinium Retention in the Central and Peripheral Nervous System: Implications for Pain, Cognition, and Neurogenesis. *Radiology*, 192645 (2020).
61. Fang P, Yu M, He B *et al.* Central injection of GALR1 agonist M617 attenuates diabetic rat skeletal muscle insulin resistance through the Akt/AS160/GLUT4 pathway. *Mech Ageing Dev*, 162, 122-128 (2017).
62. Wen S-Y, Chen Y-Y, Deng C-M, Zhang C-Q, Jiang M-M. Nergoside suppresses colorectal cancer cell growth and metastatic potential through inhibition of ERK/GSK3 β / β -catenin signaling pathway. *Phytomedicine*, 57, 352-363 (2019).
63. Huang B-R, Bau D-T, Chen T-S *et al.* Pro-Inflammatory Stimuli Influence Expression of Intercellular Adhesion Molecule 1 in Human Anulus Fibrosus Cells through FAK/ERK/GSK3 and PKC δ Signaling Pathways. *Int J Mol Sci*, 20(1) (2018).
64. Zakharova IO, Sokolova TV, Bayunova LV *et al.* The Protective Effect of Insulin on Rat Cortical Neurons in Oxidative Stress and Its Dependence on the Modulation of Akt, GSK-3 β , ERK1/2, and AMPK Activities. *Int J Mol Sci*, 20(15) (2019).
65. Brauns-Schubert P, Schubert F, Wissler M *et al.* CDK9-mediated phosphorylation controls the interaction of TIP60 with the transcriptional machinery. *EMBO Rep*, 19(2), 244-256 (2018).
66. Charvet C, Wissler M, Brauns-Schubert P *et al.* Phosphorylation of Tip60 by GSK-3 determines the induction of PUMA and apoptosis by p53. *Mol Cell*, 42(5), 584-596 (2011).
67. Nayak G, Cooper GM. p53 is a major component of the transcriptional and apoptotic program regulated by PI 3-kinase/Akt/GSK3 signaling. *Cell Death Dis*, 3, e400 (2012).

Publisher's Note Springer Nature remains neutral with regard to jurisdictional claims in published maps and institutional affiliations.